https://doi.org/10.2352/ISSN.2470-1173.2017.14.HVEI-134

Characterization of Spatiotemporal Fluctuation in Absorbed Light Energy by an Array of Interleaved Photosensitive Elements

Shahram Peyvandi [a], Vebjørn Ekroll [b], Alan Gilchrist [a]; [a] Department of Psychology, Rutgers, The State University of New Jersey, Newark, New Jersey 07102, USA. [b] Laboratory of Experimental Psychology, University of Leuven (KU Leuven), Belgium.

Abstract

The electrical activity in a photoreceptor is initiated when photons are absorbed by photopigment molecules of the cell. When the receptor is exposed to a photon flux of a particular wavelength, the actual number of photons absorbed in a cell varies with Poisson fluctuation. This fluctuation introduces a spatial variation in absorption by cells and a temporal variation, with repeated exposure, in the number of cells absorbing each specific level of light energy. Here we characterize such variations and quantify the relationship between the spatial and temporal variations for an array of receptors exposed to an arbitrary light spectrum. The spatial variation in absorption by cone cells implies that visual stimulation produces a distribution of responses in cone excitation space. We show that the resulting excitations directly reproduce MacAdam's (1942) classic measurements of the variability of color matches. Our model applies to both a living and a non-living array of photosensitive elements. We carried out a performance evaluation by a CMOS sensor repeatedly exposed to uniformly illuminated color patches. Our findings suggest that spatial fluctuation in absorbed light energy by cells is invariant with respect to the total number of like-type cells from which the histogram is obtained. However, temporal variation with repeated exposure in the proportion of cells at a specific level of absorbed light energy decreases as the spatial variance and number of pixels increases. Our results also support the assumption that each cell absorbs light energy independently from the other cells. The proposed characterization is important for understanding the retinal factors that limit color detection and discrimination in the human visual system. It also has technical significance for color image enhancement in imaging by a digital sensor.

Introduction

When a photoreceptor is exposed to a photon flux of a particular wavelength, the stochastic nature of absorbed light energy is described by the probability that a particular number of photons is absorbed in the receptor. The actual number of photons absorbed in a cell varies with Poisson fluctuation. This type of fluctuation, known as photon noise [1], has been investigated in retinal receptors of the human eye [2–4] and digital camera sensors [5–7]. This photon fluctuation, however, should be revisited for the case in which a population of receptors is exposed repeatedly to arbitrary light of multiple wavelengths. This is because, first, due to the principle of univariance [8], spatial variation in the excitation of cells is described by the variance of absorbed light energy among a population of identical cells of a specific type and not by the variability in the number of photons absorbed in a cell. Second, with repeated exposures, the relation between temporal variation in the number of cells at a given energy level and the spatial variation in absorption by a population of cells is not specified merely by the distribution of photons in a cell.

In this paper, we determine a distribution for the average number of cells at each specific level of absorbed light energy, the variance of which quantifies the spatial variation in absorption by individual cells. With repeated exposure, we also determine the temporal fluctuation in the number of cells absorbing an energy level and discuss the relation between the spatial and temporal variations. To validate this relationship, we carry out a performance evaluation on a CMOS sensor.

Distribution of Cells across Energy Levels

The fundamental assumptions and mathematical derivations underlying the proposed model are provided elsewhere [9]. Here we introduce a distribution for the absorbed light energy by a population of photoreceptor cells. When a retinal area containing N identical cells of the same class is stimulated with light of multiple frequencies, with the assumption that N cells absorb photons of different frequencies independent from each other,

$$\mathrm{d}\bar{N}_Q \approx \frac{N}{\sigma_Q\sqrt{2\pi}} \exp\left[-\frac{1}{2}\Big(\frac{Q-\mu_Q}{\sigma_Q}\Big)^2\right] \mathrm{d}Q \;;\; Q \geq 0, \qquad (1)$$

represents the average number of cells, $\mathrm{d}\bar{N}_Q$, that have absorbed photon energy between Q and $Q+\mathrm{d}Q$ units. In Eq. (1),

$$\begin{aligned} \mu_Q &= \frac{\varrho\, A\,\Delta t}{f^2} \int_\nu \tau_\nu J_\nu I_\nu \,\mathrm{d}\nu\,, \\ \sigma_Q^2 &= h\,\frac{\varrho\, A\,\Delta t}{f^2} \int_\nu \nu\,\tau_\nu J_\nu I_\nu \,\mathrm{d}\nu\,. \end{aligned} \qquad (2)$$

The parameters of the model are listed in Table 1. Figure 1(a) schematically illustrates the spatiotemporal variation. In Eq. (2), μ_Q is the average amounts of light energy absorbed by N identical cells all together, and σ_Q^2 is the spatial variance in the amount of energy absorbed by all N cells. In this model, N_Q is the number of identical cells with energies between Q and $Q \pm \Delta Q/2$, for an instance of exposure. The actual amount of absorbed energy in a cell varies with repeated exposure, causing a temporal fluctuation in the histogram itself. We are also interested in finding $var(N_Q)$, the temporal variation, with repeated exposure, in the number of cells with Q units of energy, that is,

$$var(N_Q) = \bar{N}_Q(1-\bar{N}_Q/N). \qquad (3)$$

Within a small energy interval, δQ, the temporal variance in the proportion of identical cells with μ_Q energy units is approximated by,

$$var(N_{\mu_Q}/N) \approx \frac{\delta Q}{N\sigma_Q\sqrt{2\pi}}. \quad (4)$$

Table 1. The table summarizes a list of parameters for estimating the histogram of absorption in Eq. (1).

Parameter	Description	Units
ν	Frequency	Hz
h	The Plank Constant	J s
I_ν	Stimulating spectral radiance	$\mathrm{W\,sr^{-1}\,m^{-2}\,Hz^{-1}}$
ϱ	Collecting area of a photoreceptor	$\mathrm{m^2}$
A	Pupil area	$\mathrm{mm^2}$
f	Focal length of the eye	mm
τ_ν	Pre-retinal spectral transmittance	–
J_ν	Spectral absorptance of a cell	–
Q	Level of energy	J
N	The total number stimulated cells	–
N_Q	Number of cells with Q energy units	–
$\bar{N}_Q$	Expected number of cells with Q energy units	–
μ_Q	Average of absorbed energy by all the N cells	J
σ_Q^2	The spatial variance	$\mathrm{J^2}$
$var(N_Q)$	The temporal variance	–
Δt	Duration of exposure	s

Distribution of Cone Excitations in Color Space

Given that identical cells exposed to uniform light absorb different levels of energy, our model can predict, as shown in Figure 1(a), the distribution of responses within cone excitation space produced by trichromatic stimulation. Such scattering, at least at the moment of receptoral stimulation, implies an uncertainty due to spatial variation in absorption by individual cells [10, 11]. Previous studies [12, 13] suggest that this uncertainty may influence human color discrimination performance. To illustrate such scatterings, we selected 25 color centers of MacAdam ellipses [14]. The spectral radiance of a color at the luminance of $50\,\mathrm{cd\,m^{-2}}$ is produced by a mixture of three Gaussian-shaped virtual primaries with the center wavelengths of 455, 520, 650 nm and a FWHM of 30 nm. For the purpose of illustration, we take Δt = 1 s and ϱ = 2 $\mu\mathrm{m}^2$, and use the Smith and Pokorny cone fundamentals [15]. As shown in Code File 1 [16], we used the Monte Carlo method to randomly generate excitations in the three types of cone cells using Eq. (1). Figure 1(b) shows the distribution of cone excitations for each of the 25 MacAdam color stimuli in the MacLeod-Boynton chromaticity diagram [17]. Note that the chromaticity coordinates, l and s in this plot are not independent variables: Their joint probability follows a form of ratio distribution [18]. The distribution of cone excitations represented within the Judd modified CIE 1931 chromaticity space in Figure 1(c) closely resemble those of the magnified chromaticity scatterings obtained by MacAdam for the variability of color matches. This observation is not trivial because the distribution of chromaticities for a color stimulus is directly obtained from the corresponding cone excitations and it also supports the notion of a probabilistic representation of color within a color space rather than a deterministic one [19]. Note that evidence for the contribution of higher order mechanisms, such as sites of adaptation, to the discriminability judgment has also been reported in the literatures (for reviews see [20, 21]). The result shown here motivates further investigation into the influence of individual cell signals on the discrimination mechanism and the source of observed differences between the variability of color matches and discrimination threshold (see p. 574 in [22]).

Digital Sensor

The proposed distribution of photon energies among photoreceptors applies equally to a non-living array of photosensitive elements. In a digital sensor, J_ν in Eq. (2) is equivalent to the spectral quantum efficiency function, τ_ν is the spectral transmittance of the lens, f is the distance from the lens to the image plane, ϱ is the effective pixel area, A is the effective aperture size and Δt is the duration of exposure. By taking the charge, q, collected by each pixel across wavelengths as a variable, we have:

$$\begin{aligned} \mu_q &= q_0 \frac{\varrho\, A\, \Delta t}{f^2} \int_\nu \tau_\nu \frac{J_\nu}{h\nu} I_\nu \,\mathrm{d}\nu\,, \\ \sigma_q^2 &= q_0^2 \frac{\varrho\, A\, \Delta t}{f^2} \int_\nu \tau_\nu \frac{J_\nu}{h\nu} I_\nu \,\mathrm{d}\nu\,, \end{aligned} \quad (5)$$

in which, q_0 is the charge of an electron. From Eq. (4), we find the relationship between the temporal and spatial fluctuations at the peak of average μ_q as

$$var(N_{\mu_q}/N) \approx \frac{\delta q}{N\sigma_q\sqrt{2\pi}}, \quad (6)$$

in which $var(N_{\mu_q}/N)$ is the temporal variance in the proportion of pixels with the average collected charge of μ_q.

Experiment

Since the proposed model applies to an array of pixels as well, we expect that the model predicts accurately the relationship between the spatial and temporal fluctuations in a digital sensor, as given in Eq. (6).

Method

A CMOS sensor was repeatedly exposed to a uniformly illuminated Macbeth color checker with 24 color patches. The spectral radiance for each of the 24 color patches was measured by a PR650 spectroradiometer. Acquisition of an unprocessed raw RGGB image was performed with an exposure duration of 50 ms. To account for the dark voltage, a dark pedestal value of 42 bits was taken off from the raw image pixel values. Figure 2 shows the experimental setup and the spectral quantum efficiency functions of the imaging device modified by transmittance of the lens.

Results

The histogram distributions of 10-bit digital output of the sensor with repeated exposure is plotted separately for each of the RGGB channels by black curves in Figure 3(a). In this plot, a

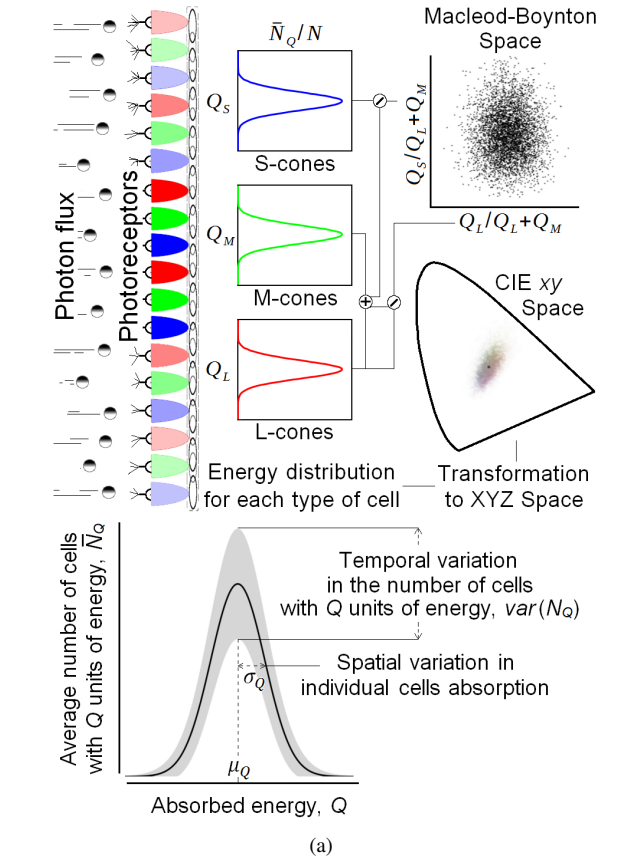

Figure 1. *Our model suggests that identical cells within a cone class (L-, M-, or S-cone) exposed to uniform stimulating light absorb different levels of light energy. Due to spatial variation, a visual stimulation produces a distribution of responses within the cone excitation space. (a) The histogram of the average number of cells with Q units of absorbed energy, $\bar{N}_Q$, approximately follows a form of Gaussian distribution. The proportion of like-type cells is shown by $\bar{N}_Q/N$. The gray region around the black distribution curve shows the temporal variation in the number of cells at an energy level. (b) A Monte Carlo simulation of excitations in cone cells exposed to the 25 MacAdam color stimuli shown within the MacLeod-Boynton chromaticity diagram. The diagram is plotted by $(l,s) = (Q_L/Q_L+Q_M\,,\, Q_S/Q_L+Q_M)$ where Q_L, Q_M, and Q_S are independently generated random energies for L-, M-, and S-cones, respectively. (c) Assuming that the cone responses are linearly related to the color-matching functions, the triplet, (Q_L, Q_M, Q_S), is linearly transformed to the Judd modified CIE 1931 XYZ space from which distributions for the same 25 stimuli are plotted within the xy chromaticity space (see p. 615 ref. [22]).*

solid colored curve shows the distribution predicted by the model. The temporal variation in the number of pixels at each specific level of digital count can be observed by histogram fluctuation along the vertical axis. As shown in Figure 3(b), the model predicts such temporal fluctuation quite accurately.

To illustrate the results obtained with repeated exposures, we measured the average of pixel values and the spatial variance of pixel values for each of the 24 color patches across trials of exposure, from which the transformation-invariant quantity of the channel-wise signal-to-noise ratio (SNR: mean divided by the standard deviation) was calculated for each of the 24 color patches. We plot in Figure 4(a) the measured SNR as a function of the predicted SNR (μ_q/σ_q). In this plot, the fluctuation along the

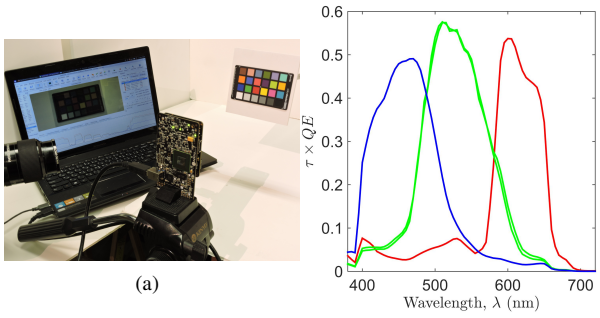

Figure 2. *In the experiment, a CMOS digital sensor with 10-bit digital output was exposed repeatedly to a uniformly illuminated color checker. (a) The figure shows the experimental setup. (b) The quantum efficiency function of the sensor, QE, corrected for the transmittance of the lens, τ, is plotted as a function of wavelength for each of the sensor channels.*

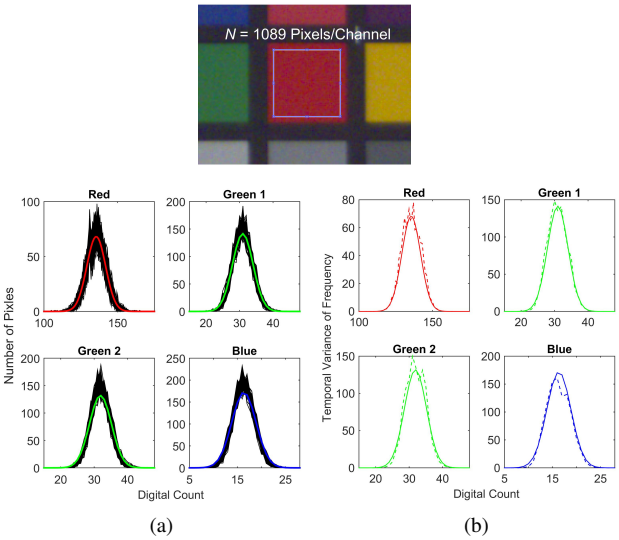

Figure 3. *A CMOS sensor was repeatedly exposed to a small color checker. In each trial of exposure, the histogram of pixel values was obtained from an array of 1089 pixels per channel. For a color patch, we predicted the mean and variance of the charge collected by pixels using Eq. (5). We then perform a linear transformation to plot the predicted distribution centered on the average of pixel values for each of the RGGB channels. (a) The channel-wise histogram across trials of exposure for a red patch is shown by black curves. The solid colored curve is the predicted distribution. (b) The measured temporal variance with repeated exposure is plotted by a dashed curve. In this plot, the predicted temporal variance is shown by a solid curve.*

vertical axes is due to the temporal variation of histogram distribution across trials of exposure. This result represents the typical performance of the model in predicting the histogram for a single exposure, despite fluctuation in the actual amount of absorbed energy by a cell. However, as shown in Eq. (1), the model predicts the expected value of the number of cells at each energy level with repeated exposure. Therefore, we carry out performance evaluation by comparing the prediction with the average of histograms obtained with repeated exposures. From the average histograms for a given color patch, we plotted the measured SNR versus the predicted SNR for each of the RGGB channels in Figure 4(b). Visual inspection of the plots in Figure 4 illustrates the performance of the model.

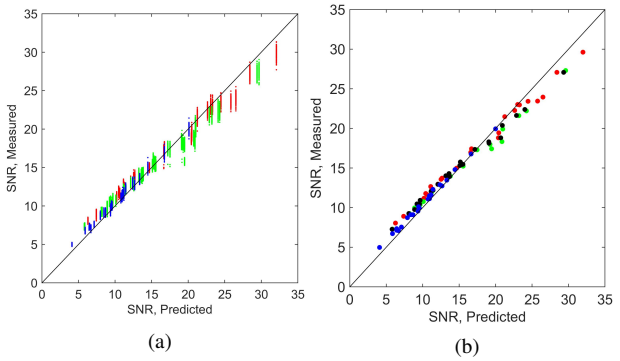

Figure 4. *For each of the 24 color patches across trials of exposure, an area with 1089 pixels per channel was selected and the mean of pixel values as well as the variance of the same patch was calculated. (a) The plot shows the measured SNR, the mean of pixel values divided by the standard deviation of the same patch, across trials of exposure as a function of the predicted SNR (μ_q/σ_q) for each of the RGGB sensor channels. The observed fluctuations along the vertical axis correspond to the temporal variation with repeated exposure in the number of pixels at each specific level of digital counts. (b) From the average histograms of a color patch, we obtain the mean divided by the standard deviation of the same patch (SNR). The plot shows the measured SNR as a function the predicted SNR.*

The Relation Between Spatial and Temporal Variations

As shown for a red color patch in Figure 3, the histogram of pixel values fluctuates with repeated exposure. This type of temporal fluctuation, $var(N_Q)$, corresponds to the variation of the number of pixels at each specific level of absorbed light energy. Note that digital outputs from a sensor are also subject to signal-independent noise [23] which causes shifts in the histogram itself with repeated exposure. The unimodal distribution of the temporal variance in Figure 3(b) shows that spatiotemporal variations of the sensor signals in our setup is not appreciably influenced by such sensor-based noises. According to Eq. (6), the temporal fluctuation is reciprocally related to the spatial variation of light energy absorbed by individual cells. To illustrate such dependency, for each of the 24 color patches, we measured the variance of the proportion of like-type pixels with average value across trials of exposure. We also measure standard deviation of the channel-wise pixel values within a color patch using the average of histograms obtained from repeated exposure. The total number of pixels per channel, N, is 1089. We expect that Eq. (6) predicts the measured temporal variance at the peak of average, $var(N_{\mu_q}/N)$, from the standard deviation of pixel values. The result is shown by a black curve in Figure 5. The dependency of temporal variation upon the spatial variance implies that Eq. (1) provides more accurate prediction of the histogram distribution for an instance of exposure to a color patch when the spatial variance has greater values. A similar reciprocal relationship can be observed in Eqs (4) and (6) between the temporal variance and the total number of pixels, N.

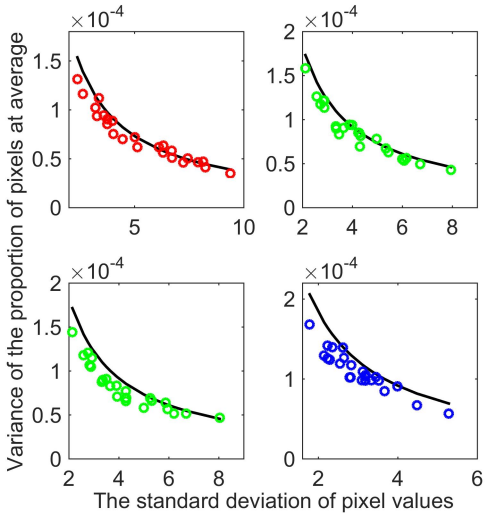

Figure 5. *For each of the 24 color patches and each of the four sensor channels, we measured the variance of the proportion of pixels with average value across trials of exposure. The figure shows a scatterplot of the measured temporal variance for the 24 patches against the measured standard deviation of the channel-wise pixel values within the same patch. The total number of pixels per channel, N, is 1089. The prediction by Eq. (6) is shown by a black curve.*

Discussion

We have proposed a distribution for absorbed light energy among a population of identical photosensitive elements, applicable to retinal photoreceptors and an array of interleaved pixels in a digital sensor. Our model accounts for the spatial variation in absorption by a population of cells and the temporal variation in the number of cells at a specific level of light energy. The spatial variation implies that visual stimulation produces a distribution of responses in cone excitation space. We showed that the resulting excitations in individual cone cells directly reproduce MacAdams classic measurements of the variability of color matches [14].

The temporal variance in the number of cells having absorbed Q units of energy, $var(N_Q)$, depends on the spatial variance and number of cells from which the distribution is obtained. A possible behavioral consequence of such variation is the perceptual uncertainty in perceived color for small stimuli [24, 25] where color is reconstructed from noisy input signals [26]. In this case, an excitation falling well beyond the nominal chromaticity gamut might be classified by an observer as an *indescribable* color when neighboring cells receive very low level of light energy (dark background) [25]. When many neighboring cells receive stimulation well above threshold level (dimly illuminated background) [27], such out-of-gamut colors are possibly very unlikely to occur. Further investigation, however, is required to validate this assumption by direct observation from the human retina.

Variability in the absorptance of individual cones was also observed in microscopic images of the human retina [28] which was found to be primarily related to the intrinsic fluctuation in reflectance of photoreceptors [29, 30]. In the digital domain, a CMOS sensor suffers from photo-response non-uniformities and gain variation [31]. Thus the spatial variation of digital outputs in a sensor is partly attributed to such non-uniformities. We expect that the proposed characterization helps to identify and decompose sources of spatiotemporal variations in a sensor output signals.

Conclusion

We characterized the spatiotemporal variation in absorption by cells when a population of receptors is exposed repeatedly to a uniform radiation of multiple wavelengths. The proposed model suggests a probabilistic representation of color within a color space rather than a deterministic representation of color by light vectors. The characterization of such probabilistic representation provides further dimensions which facilitate color image enhancement and the analysis of the illumination using digital outputs of a sensor [32–34]. Although, our results confirmed the performance of the model in a CMOS sensor, we acknowledge that further investigation is required to evaluate signal fluctuation due to spatial non-uniformities and intrinsic variation in optical specifications of an imaging system.

Acknowledgments

We are thankful to James Tornes and Manjunath Somayaji from ON Semiconductor for providing us with the CMOS sensor. We also acknowledge Sunex, Inc. for providing the spectral transmittance of the lens.

Funding Information

SP and AG were supported by National Science Foundation (NSF) (BCS-1230793); VE was supported by a travel grant from the FWO (FN14409) and the Methusalem program by the Flemish Government (METH/08/02 and METH/14/02), awarded to Johan Wagemans.

References

[1] S. W. Hasinoff. Photon, poisson noise. In I. Ikeuchi, editor, *Computer Vision: A Reference Guide*, pages 608–610. Springer, New York, 2014.

[2] M. A. Bouman, J. J. Vos, and P. L. Walraven. Fluctuation theory of luminance and chromaticity discrimination. *J. Opt. Soc. Am.*, 53(1):121–128, 1963.

[3] W. Geisler. Sequential ideal-observer analysis of visual discrimination. *Psychol. Rev.*, 96(2):267–314, 1989.

[4] F. Rieke and D. A. Baylor. Single-photon detection by rod cells of the retina. *Rev. Mod. Phys.*, 70(3):1027–1036, 1998.

[5] H. Kuniba and R. S. Berns. Spectral sensitivity optimization of color image sensors considering photon shot noise. *J. Electron. Imaging*, 18(2):023002, 2009.

[6] J. E. Farrell, P. B. Catrysse, and B. A. Wandell. Digital camera simulation. *Appl. Opt.*, 51(4):A80–A90, 2012.

[7] R. Costantini and S. Susstrunk. Virtual sensor design. In *Proc. SPIE*, volume 5301, pages 408–419, 2004.

[8] W. A. H. Rushton. Pigments and signals in colour vision. *J. Physiol.*, 220(3):1–31P, 1972.

[9] S. Peyvandi. PhD thesis, Department of Psychology, Rutgers, The State University of New Jersey, Newark, USA, 2017.

[10] S. Peyvandi and A. Gilchrist. A new approach to the absorption of photon energy among retinal cells provides the key to some old problems in color vision. *J. Vision*, 16(12):1150, 2016.

[11] S. Peyvandi and A. Gilchrist. Does spatially homogeneous color stimulation produce a single response point within the physiological cone excitation space? In *the 16th Annual Optical Society Fall Vision Meeting*, Rochester, NY, 2016. OSA Fall Vision Meeting.

[12] D. G. Pelli. Uncertainty explains many aspects of visual contrast detection and discrimination. *J. Opt. Soc. Am. A*, 2(9):1508–1532, 1985.

[13] M. Vorobyev and D. Osorio. Receptor noise as a determinant of color thresholds. *Proc. R. Soc. Lond. B*, 265(1394):351–358, 1998.

[14] D. L. MacAdam. Visual sensitivities to color differences in daylight. *J. Opt. Soc. Am.*, 32(5):247–274, 1942.

[15] V. C. Smith and J Pokorny. Spectral sensitivity of the foveal cone photopigments between 400 and 500 nm. *Vision Res.*, 15(2):161–171, 1975.

[16] S. Peyvandi, V. Ekroll, and A. Gilchrist. MATLAB codes for the distribution of photon energy among a population of interleaved photoreceptors. `https://github.com/peyvandi/light-energy-distribution-among-photoreceptors`. [retrieved 8 Jan 2017].

[17] D. I. A. MacLeod and R. M. Boynton. Chromaticity diagram showing cone excitation by stimuli of equal luminance. *J. Opt. Soc. Am.*, 69(8):1183–1186, 1979.

[18] T. Pham-Gia, N. Turkkan, and E. Marchand. Density of the ratio of two normal random variables and applications. *Commun. Stat. Theor.*, 35(9):1569–1591, 2006.

[19] B. A. Wandell. Measurement of small color differences. *Psychol. Rev.*, 89(3):281–302, 1982.

[20] R. T. Eskew. Higher order color mechanisms: A critical review. *Vis. Res.*, 49(22):2686–2704, 2009.

[21] A. Stockman and D. H. Brainard. Fundamentals of color vision I: color processing in the eye. In A. J. Elliot, M. D. Fairchild, and A. Franklin, editors, *Handbook of Color Psychology*, pages 27–69. Cambridge University Press, 2015.

[22] G. Wyszecki and W. S. Stiles. *Color Science: Concepts and Methods, Quantitative Data and Formula*. John Wiley & Sons, NY, 1982.

[23] S. Peyvandi, S. H. Amirshahi, J. Hernández-Andrés, J. Romero, and J. L. Nieves. Generalized inverse-approach model for spectral-signal recovery. *IEEE Trans. Image Process.*, 22(2):501–510, 2013.

[24] J. Krauskopf. Color appearance of small stimuli and the spatial distribution of color receptors. *J. Opt. Soc. Am.*, 54(9):1171, 1964.

[25] H. Hofer, B. Singer, and D. R. Williams. Different sensations from cones with the same photopigment. *J. Vision*, 5(5):5, 2005.

[26] D. H. Brainard, R. W. Williams, and H. Hofer. Trichromatic reconstruction from the interleaved cone mosaic: Bayesian model and the color appearance of small spots. *J. Vision*, 8(5):15, 2008.

[27] R. Sabesan, B. P. Schmidt, W. S. Tuten, and A. Roorda. The elementary representation of spatial and color vision in the human retina. *Sci. Adv.*, 2(9):e1600797, 2016.

[28] A. Roorda and D. R. Williams. The arrangement of the three cone classes in the living human eye. *Nature*, 397:520–522, 1999.

[29] A. Pallikaris, D. R. Williams, and H. Hofer. The reflectance of single cones in the living human eye. *Invest. Ophthalmol. Vis. Sci.*, 44(10):4580–4592, 2003.

[30] R. F. Cooper, A. M. Dubis, A. Pavaskar, J. Rha, A. Dubra, and J. Car-

roll. Spatial and temporal variation of rod photoreceptor reflectance in the human retina. *Biomed. Opt. Express.*, 2(9):2577–2589, 2011.

[31] J. Nakamura. *Image Sensor and Signal Processing for Digital Still Cameras*. CRC Press, FL, USA, 2006.

[32] S. Peyvandi, J. L. Nieves, and A. Gilchrist. On the information content along edges in trichromatic images. In *CIC21, 21st Color and Imaging Conference*, pages 236–239, Albuquerque, New Mexico, 2013. IS&T and SID.

[33] D. Cheng, D. K. Prasad, and M. S. Brown. Illuminant estimation for color constancy: why spatial-domain methods work and the role of the color distribution. *J. Opt. Soc. Am. A*, 31(5):1049–1058, 2014.

[34] S. M. C. Nascimento, K. Amano, and D. H. Foster. Spatial distributions of local illumination color in natural scenes. *Vision Res.*, 120:39–44, 2016.

Author Biography

Shahram Peyvandi received his PhD in color science from Amirkabir University of Technology (Tehran Polytechnic) in 2012. He is currently a PhD candidate in color perception and cognition at the Department of Psychology at Rutgers University, Newark. His current research focuses on the distribution of photon energy among retinal photoreceptors and characterization of noise in a CMOS image sensor.

Vebjørn Ekroll has a Diploma in Psychology (Dipl. Psych.) from the University of Kiel, where he also earned his Doctorate (Dr. phil.) and completed his Habilitation (Dr. habil.). He is currently a postdoctoral researcher at the Laboratory of Experimental Psychology in Leuven. His research focuses on various topics such as color perception, motion perception, amodal completion, and the psychology of magic is motivated by a more general interest in perceptual organization and the structure of perceptual representations.

Alan Gilchrist received his BA in Psychology from Portland State University and the PhD from Rutgers University in 1975. After a postdoctoral fellowship at Bell Laboratories, he spent five years at Stony Brook University before returning to Rutgers in 1981. He conducts research on the perception of surface lightness and color. He is the founder of Club Vision, a Consulting Editor of Perception/i-Perception, the Editor of Lightness, Brightness and Transparency (1994), and the author of Seeing Black and White (2006).